

## METHODS

# The Seamless Transition From Discrete Frequency Control to Phase Control Method Using Soft Starter

POOREUM JANG<sup>1b</sup>, BYONG JO HYON<sup>1b</sup>, DAE YEON HWANG, JOON SUNG PARK<sup>1b</sup>, JUN-HYUK CHOI, AND JIN-HONG KIM

Korea Electronics Technology Institute, Bucheon-si 13509, South Korea

Corresponding author: Jin-Hong Kim (kimjinghong@keti.re.kr)

This work was supported by the Korea Institute of Energy Technology Evaluation and Planning (KETEP) funded by the Korean Government (MOTIE) through the Development and Demonstration of an Integrated Energy and Environment Management System (EEMS) for Manufacturing under Grant 2022202090003B.

**ABSTRACT** Soft starters are used in a variety of industries to safely apply grid voltage to drive induction motors. The soft starter protect the motor from overcurrent and torque that occurs during starting of the motors by regulating the voltage applied to the motor. There are various methods to implement this soft starter, and among them, the discrete frequency control (DFC) method allows for simple operation, but research to limit the motor peak current is still insufficient. In this paper, a new method to limit the current and start the induction motor using the DFC was proposed. The proposed method calculates the feedforward component of the firing angle according to the speed command and add it to the output of additional controller to limit the current. The proposed method has the advantage of seamless transition to the phase control method when the speed command increases and can be implemented without structural change from the conventional phase control method. Using this method, it is implemented without motor parameter information, and the system efficiency is improved. The effectiveness of proposed method was verified through simulations and experiments.

**INDEX TERMS** Soft starter, discrete frequency control (DFC), efficiency, induction motor.

## I. INTRODUCTION

Electric motors are used in a variety of industries and their efficiency are so important because they account for roughly half of global electricity consumption. In particular, as the problem of environmental pollution due to carbon emissions has recently received a lot of attention, various studies are being conducted to improve the efficiency of electric motors and power conversion devices that drive the motors. There are various types of electric motors, but permanent magnet synchronous motor (PMSM) is frequently used in electric propulsion systems such as electric vehicles and urban air mobilitys (UAMs) due to its high power density and efficiency. Although much research is being conducted on

electric propulsion systems using PMSM, induction motors (IMs), which are easy to maintain, account for a larger portion of motor usage across industries such as conveyors and pumps.

Inverters are often used to drive these electric motors. The inverter can be configured in various ways, such as 2-level or 3-level, depending on the voltage level [1], [2]. To control the motors, it use pulse width modulation (PWM) to apply the desired voltage to the motor [3]. Various research is being conducted to improve the efficiency of motor systems using such inverters. In [4], it was proposed to output maximum torque while minimizing copper loss. This method operates at a minimum current magnitude that minimizes copper loss. In [5], the PWM frequency was varying according to operating point, considering not only motor loss but also inverter loss. In addition, various studies

The associate editor coordinating the review of this manuscript and approving it for publication was Jahangir Hossain<sup>1b</sup>.

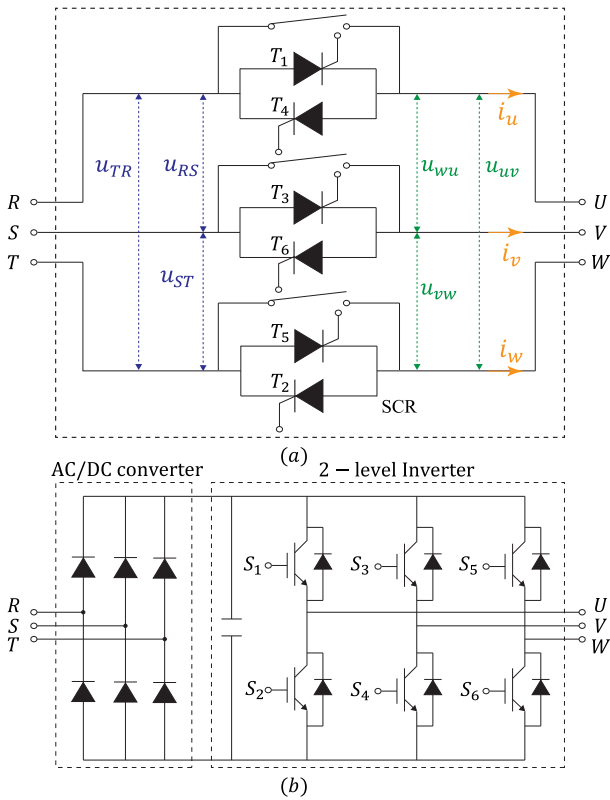


FIGURE 1. Structure of each device that drives the motor: (a) soft starter, (b) 2-level inverter.

TABLE 1. Comparison between soft starter between 2-level inverter.

Name	Soft starter	Inverter
Number of switch	6	6
Number of components	↑	↓
Need of AC/DC converter	Yes	No
Cost	Expensive	Inexpensive
Speed range	All region	Grid frequency
Input voltage	DC	AC

related to improving efficiency are being conducted, such as a driving method that considers the iron loss of the motor [6] and changing the operating point based on motor parameter estimation through signal injection [7]. Using this inverter, it is possible to operate at optimal current points to improve system efficiency, but has the disadvantage of cost for facility construction and requiring a separate AC/DC converter to supply DC-link voltage.

Soft starters are commonly used in IMs. Since these IMs account for more than 90 percent of total motor usage, such grid-connected motor drive technology is very important. Therefore, research using these soft starters is still in progress [8], [9]. In particular, they are widely used in numerous industrial manufacturing in various fields that use medium voltage, such as fans, blowers, submersible AC motors. Since the frequency of the grid voltage is constant, the operating point of the motor is relatively constant when using soft starters. To drive a motor using soft starters, there are phase control method [10], [11], [12], predictive control

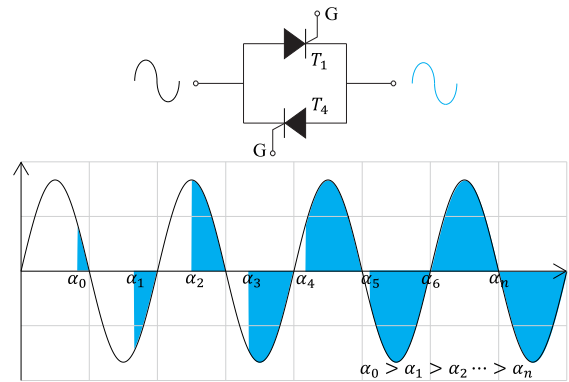


FIGURE 2. Output voltage change according to the firing angle of the thyristor.

method [13], [14], and DFC method [15], [16], [17]. In [10], a method of gradually increasing the applied voltage based on the preset rise time was proposed. Similarly, in [11], a method that measure motor current and use a controller to prevent the overcurrent was proposed. These phase control method has the advantage of easy implementation because it does not require motor parameters or other information, but it has the disadvantage that system efficiency and the magnitude of the current generated during startup vary depending on the motor. Unlike the phase control, the predictive control method basically assumes that two of the three phases are conducting, and uses the motor parameters to predict the maximum current, flux, torque, etc. of the motor, and determine whether these predicted values are within an acceptable limit [13]. This method can increase efficiency by minimizing losses because only two phases are used, but it has the disadvantage of requiring the motor parameters to be known in advance. In [15], [16], and [17], a method of dividing the grid frequency and applying it to the motor was proposed. This method presented a new method that was different from existing other methods, but research on current limiting and comparing efficiency are still insufficient.

Among the various driving methods using the soft starter, the DFC method uses divided grid frequencies, so unlike the phase control method, there is a region where current is not conducted during the starting process. Because this region are similar to predictive control methods, there is a need to compare them in terms of efficiency. Also, unlike predictive control methods, it has the advantage of being easier to apply because it does not require motor parameters and speed. In this paper, a general review of the DFC method is provided, and propose a simple implementation and current limiting method using DFC method. Section II briefly introduces the structure and principles of the soft starter. In Section III, a new DFC method considering peak current is proposed. In Section IV, the effectiveness of the proposed method was verified through simulation and experiment.

## II. STRUCTURE AND PRINCIPLE OF SOFT STARTER

The soft starter consists of six thyristors connected in anti-parallel for each phase and a bypass connector, as shown

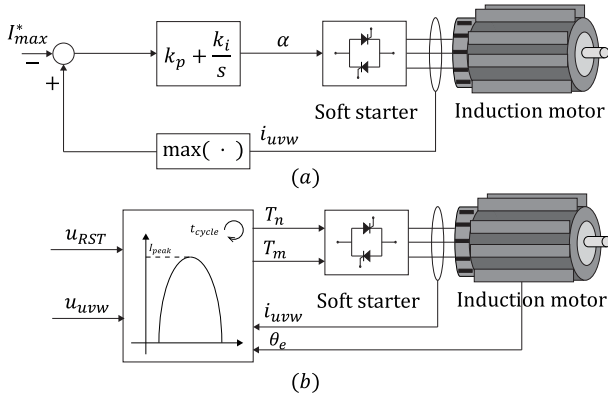


**FIGURE 3. Conventional method using soft starter: (a) phase control, (b) predictive control.**

in Fig. 1 (a). A thyristor is a silicon controlled rectifier (SCR) whose turn-on time can be adjusted by applying a gate signal. In contrast, Fig. 1 (b) shows a three-phase, two-level inverter. A three-phase inverter consists of six IGBTs or MOSFETs, DC-link capacitors, gate drivers, control boards, and AC/DC converters. Table. 1 shows the comparison between soft starters and inverters. Inverters have more components than soft starters, so they have a disadvantage of cost, but they guarantee stable performance at all speed region, so this allows operation at the maximum efficiency current point. Soft starters have the challenge of operating efficiently over the entire range, but on the other hand they have cost advantages. Recently, the use of inverters has increased in many industrial fields to increase efficiency, but soft starters are still widely used in environments where load fluctuations are small.

The voltage applied to the motor is gradually increased by adjusting the turn-on time when using soft starters. Fig. 2 shows the R phase of the soft starter in Fig. 1 (a). In Fig. 2, firing angle,  $\alpha$  means to the angle at which the gate signal is applied. When the gate signal is applied, the SCR turns on, so when the input voltage is a sine voltage, the output voltage is output such as blue curve. In other words, as  $\alpha$  is gradually reduced, the voltage applied to the motor gradually increases, and ultimately a output voltage equal to the input voltage. Based on this operating principle, over current can be prevented at the motor starting.

There are various methods to start a motor using soft starters. Typically, it can be divided into ramp methods, phase control methods, DFC methods, and predictive control methods. Among these methods, Fig. 3 (a) shows the phase control method. The phase control method measures the current of the motor and controls it so that the maximum current does not exceed the limit current. This is most commonly used because it does not require motor parameters or other information. On the other hand, Fig. 3 (b) shows the predictive control method. The predictive control basically uses two-phase conduction. This method uses the dynamics of the motor to predict the torque and current, and conducts when these predicted values are within the limit values such

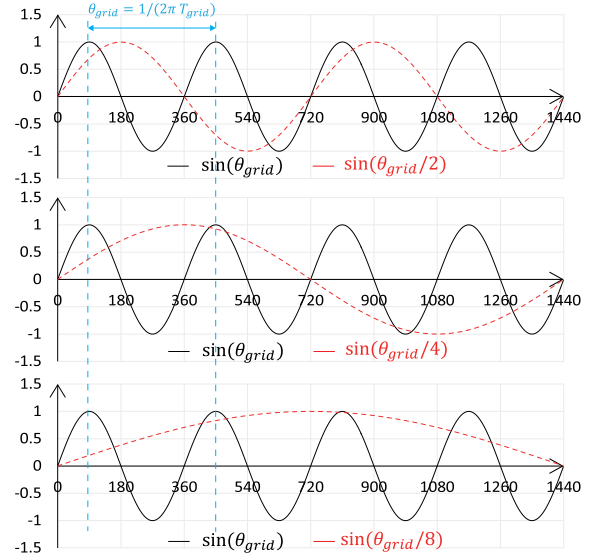


**FIGURE 4. Basic principles of DFC method.**

as current and torque. This improves system efficiency during startup and stopping because of two phases conduction. However, it have to know information of motor parameters and require a lot of calculation time.

### III. PROPOSED DISCRETE FREQUENCY CONTROL

#### A. PRINCIPAL OF DISCRETE FREQUENCY CONTROL

The DFC is a method of dividing the frequency of the grid voltage and applying a low frequency voltage to the motor. By gradually increasing the divided frequency, the speed of the motor is gradually increased to the rated speed, and finally, the grid frequency is applied. Fig. 4 shows the case where the divided low frequencies are  $f/2$ ,  $f/4$ , and  $f/8$  respectively. The divided voltage based on the grid voltage is indicated by a red dotted line. In order to apply this voltage, an appropriate gate signal must be applied to SCRs. For these gate signals, the relationship between the divided frequency and the grid frequency must be examined.

The divided frequency is expressed as follows because the grid frequency is used as input.

$$\omega_{grid} = \gamma \omega_{DFC}, \quad (1)$$

where  $\omega_{grid}$  is the grid angle velocity,  $\omega_{DFC}$  is the divided angle velocity, and  $\gamma$  is an integer representing the dividing ratio. Since the grid voltage is three-phase balanced, the divided frequency have relationship such as

$$\omega_{DFC} \cdot t - \frac{2\pi}{3} = 0, \quad \omega_{grid} \cdot t \pm \frac{2\pi}{3} = n\pi, \quad (2)$$

where  $n = 0, 2, 4 \dots$ . Using (1)-(2),  $\gamma$  and  $n$  are expressed as (3)-(4).

$$\gamma = \frac{3}{2}n + 1 \quad (\text{Positive sequence}), \quad (3)$$

$$\gamma = \frac{3}{2}n - 1 \quad (\text{Negative sequence}). \quad (4)$$

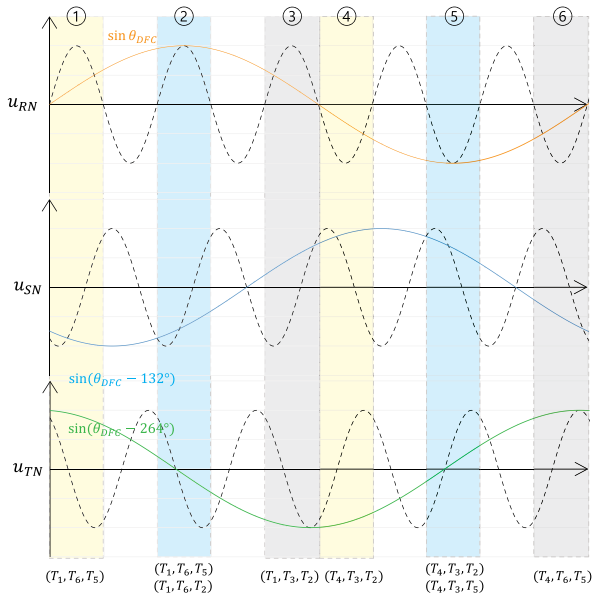


FIGURE 5. A simple method of introducing discrete frequency control.

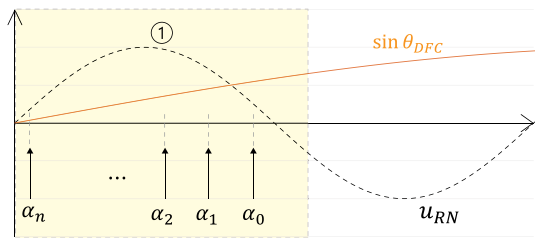


FIGURE 6. The effect of firing angle when applying discrete control method.

In a balanced system, it is expressed as (1)-(4), but the divided frequencies may be unbalanced depending on the actual motor parameters or the timing of the gate signal. Therefore, more general formula is expressed as

$$\omega_{DFC}t - \theta = 0, \tag{5}$$

$$\theta_v = \frac{(n + \frac{2}{3})}{\gamma} \pi, \quad \theta_w = \frac{(n - \frac{2}{3})}{\gamma} \pi, \tag{6}$$

where  $\theta_{v,w}$  represents the phase difference of  $v$  and  $w$  phases. According to (5)-(6), even if the divided frequency is the same, various output voltage combinations are possible according to  $\gamma$  and  $n$ . In this paper, a combination of angles with a voltage phase difference as close as possible to three-phase balance was used. It is shown in Table.2.

**B. CURRENT LIMIT METHOD FOR DFC**

There are some studies about the DFC before, but there aren't enough specific details yet on how to implement it. This section introduces a simple DFC implementation method to limit the maximum current. Fig. 5 shows the discrete frequency voltage and grid voltage when  $\gamma = 4$ . From the top, these are the voltages of the R phase, S phase, and T

TABLE 2. Phase difference between  $v$  and  $w$  phases depending on  $n$  and  $\gamma$ .

$\gamma$	v-phase angle, $\theta_v$	n	w-phase angle, $\theta_w$	n
2	150°	1	300°	4
3	100°	1	200°	4
4	120°	2	240°	6
5	132°	3	264°	8
6	110°	4	220°	10
7	120°	5	240°	11

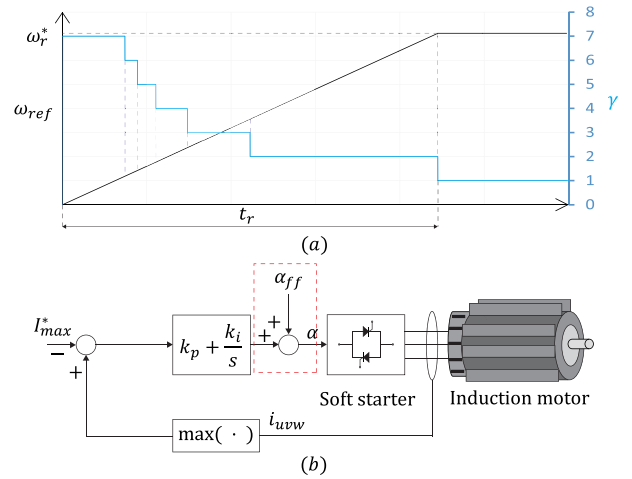


FIGURE 7. The proposed current limit method under discrete frequency control.

phase, respectively. First, looking at  $u_{RN}$  and  $u_{UN}$ , when the voltage of  $u_{UN}$  is a positive, in order for the applied voltage to be a positive,  $u_{RN}$  must also be a positive. It is expressed as areas 1, 2, and 3 in Fig. 5. Conversely, when the voltage is negative, it is areas 4, 5, and 6. The SCRs, which must determine the voltage polarity of each phase and turn on the gate signal, are shown at the bottom of the Fig. 5. In area 1,  $T_1$ ,  $T_6$ , and  $T_5$  turn on to apply positive voltage. Using this method, it is possible to simply implement DFC by determining only the signs of the grid voltage and discrete frequency voltage. It can be implemented simply because it does not require additional calculations or information, but in order to actually apply this method, it is necessary to define when the gate signal should be applied. Fig. 6 is an enlarged waveform of area 1 in Fig. 5. The motor current varies depending on the  $\alpha$ . Therefore, appropriate  $\alpha$  becomes very important to start the motor safely. In other words, even if the divided frequency is the same, the magnitude of the current varies depending on the  $\alpha$ .

Fig. 7 shows the proposed firing angle selection method. As shown in Fig. 7 (a), the speed command is increased according to the pre-specified rise time,  $t_r$ . At this time,  $\gamma$ , is calculated using the speed command. Based on  $\gamma$ , the feed forward firing angle,  $\alpha_{ff}$  to be applied according to the speed is calculated as

$$\alpha_{ff} = k \left( \frac{1 - \gamma}{\gamma_{max}} \right) + \alpha_{min}, \tag{7}$$

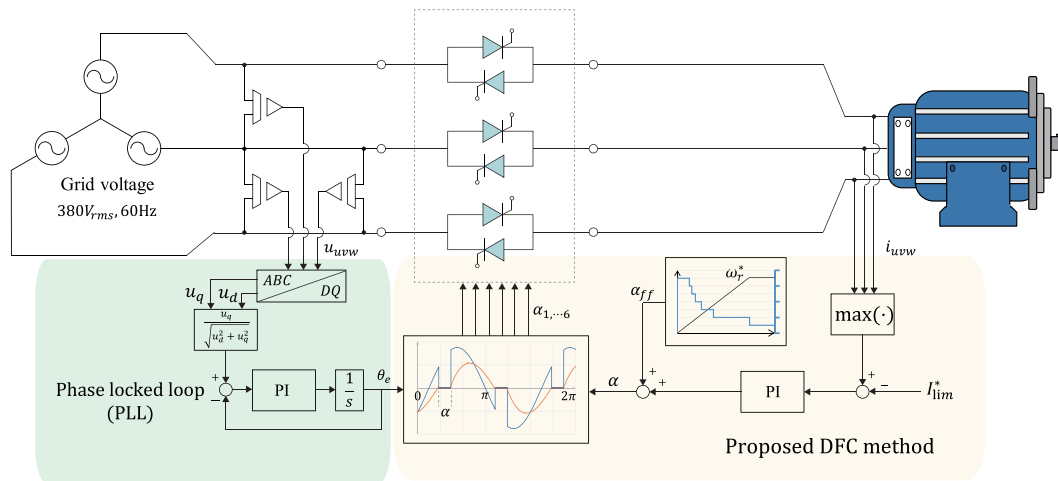


FIGURE 8. The overall block diagram of the proposed DFC method.

TABLE 3. Parameters of induction motor.

Name	Value	Unit
Rated power	1.1	kW
Rated current	1.7	A
Rated speed	1710	rpm
Number of pole, P	4	
Stator resistance, $r_s$	9.52	$\Omega$
Stator inductance, $L_s$	0.533	mH
Rotor resistance, $r_r$	8.55	$\Omega$
Rotor inductance, $L_r$	0.533	mH
Magnetizing inductance, $L_m$	0.498	mH

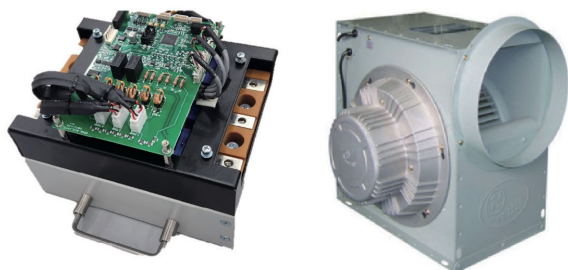


FIGURE 9. The soft starter and induction motor used in experiments.

where  $\alpha_{min}$  is final firing angle,  $\gamma_{max}$  is the maximum of  $\gamma$  and  $k$  is arbitrary constant. This means that the firing angle gradually increases depending on the speed. Using this feedforward value, the firing angle naturally increases as the speed command increases.

However, if only this feedforward value is used, over-current may occur depending on the type of motor or load situation, so additional compensation is required to safely operate the motor. Fig. 7 (b) shows a block diagram with the additional controller for current limiting. The difference between the current limit and motor current is used as input to the controller. Then feedforward value,  $\alpha_{ff}$  is added to the output. This is a combination of the existing phase control method and the ramp method. Therefore, it is possible to

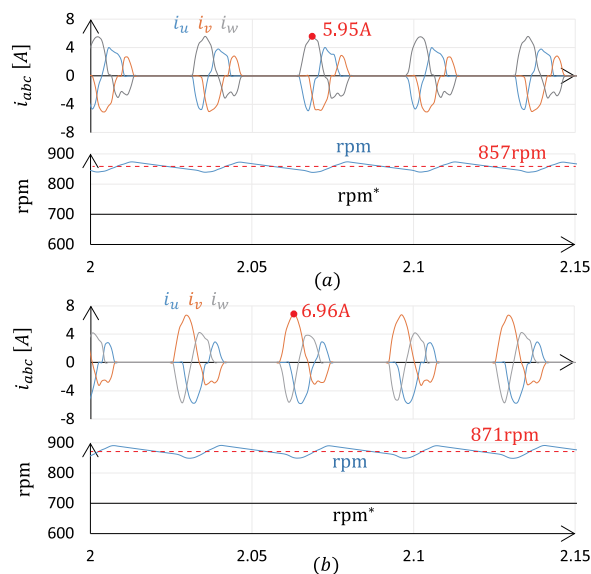


FIGURE 10. The simulation results when  $\gamma = 2$ : (a)  $\theta_v = 60^\circ$ ,  $\theta_w = 210^\circ$ , (b)  $\theta_v = 150^\circ$ ,  $\theta_w = 300^\circ$ .

simply implement the DFC method in the existing algorithm without additional motor information or speed information. In addition, in the proposed method, when  $\gamma = 1$ , the feedforward value does not change anymore, so it naturally transitions to the phase control method. The SCR can adjust the turn-on point by the gate signal and turns off according to the external load situation, so if the PI controller cycle is too fast, the current limitation may not be achieved. Therefore, the bandwidth of the PI controller must be less than the grid frequency.

#### IV. SIMULATION AND EXPERIMENT RESULTS

Fig. 8 shows the overall block diagram using the proposed method. The PLL is used based on input voltages to determine the phase of the grid voltage. At this time, gate signals are applied to the SCRs based on the  $\alpha$  of the final output using



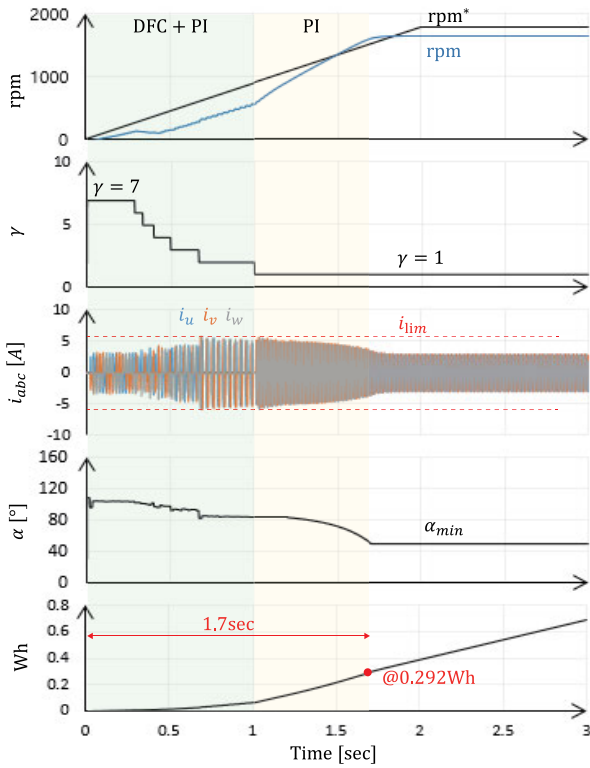


FIGURE 11. The simulation results using the proposed method.

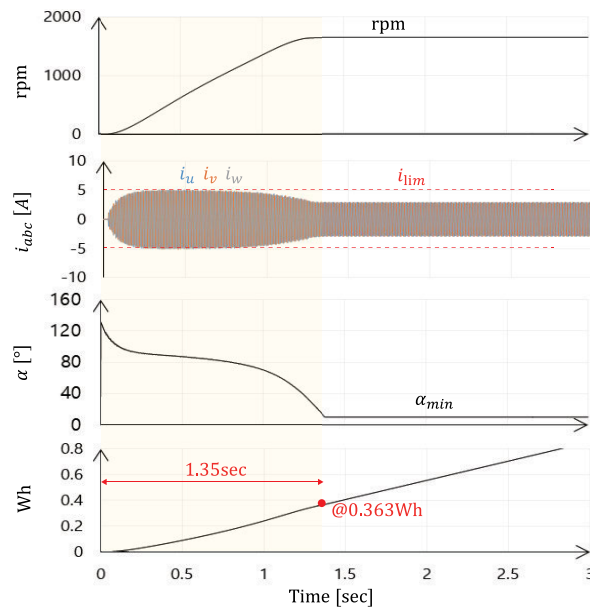


FIGURE 12. The simulation results using the phase control method.

the proposed DFC method and  $\theta_e$ . The  $\alpha_{ff}$  is calculated according to the speed command and add it to output of PI controller. Here, when  $\gamma = 1$ , this value dose not change anymore. So it switches to the phase control method to effectively limit the motor current. Using the feedforward and PI controller together, the algorithm switch DFC to phase

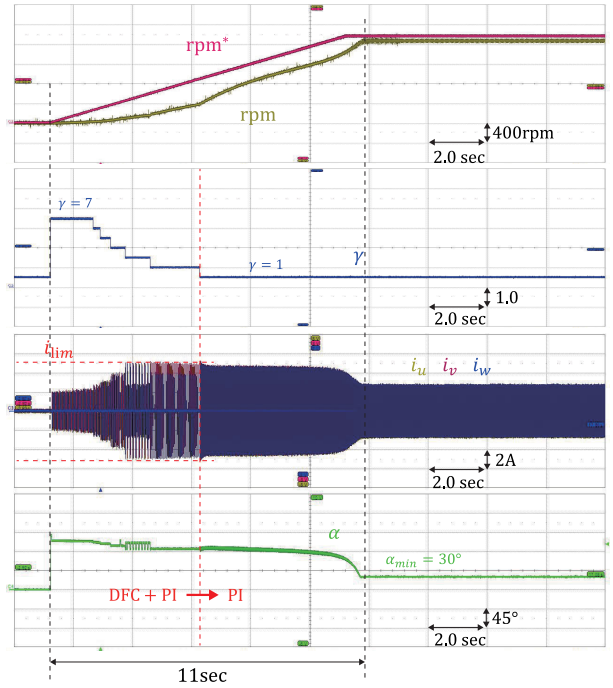


FIGURE 13. The motor speed,  $\gamma$ , motor current, and firing angle when using the proposed method.

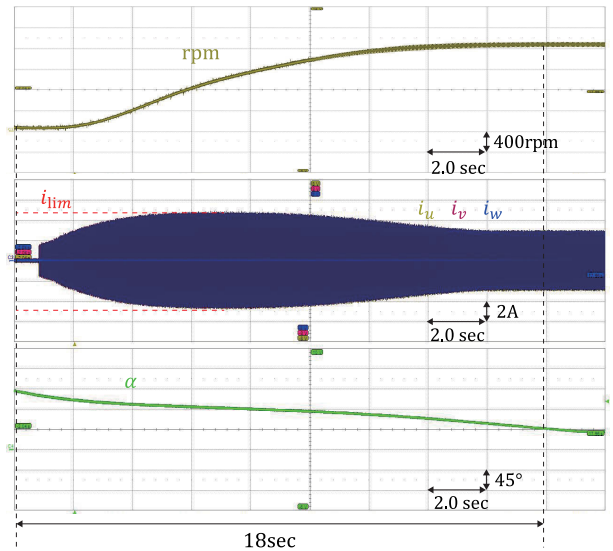
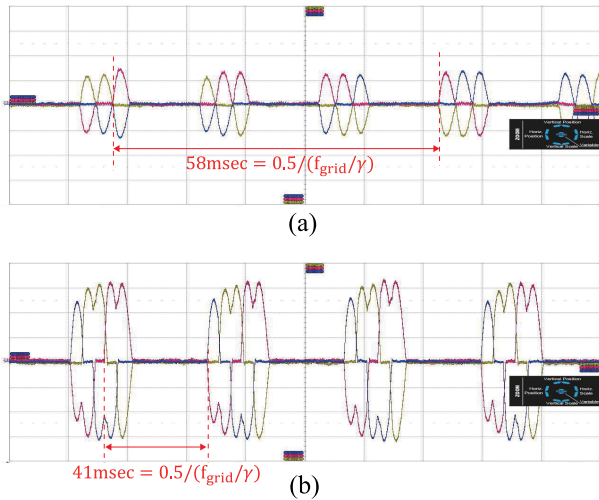


FIGURE 14. The motor speed, motor current, and firing angle when using the proposed method.

control method seamlessly. Through Fig. 7 (a), it can be seen that the interval of  $\gamma$  becomes shorter as the speed command becomes smaller. Therefore, if  $\gamma_{max}$  is set too large, the feedforward value changes frequently, so the current limiting controller may not operate properly. Therefore, selecting an appropriate  $\gamma_{max}$  is important, and in this paper,  $\gamma_{max} = 7$  was selected. The parameters of IM used in the experiments and simulations are listed in Table.3. The simulation was conducted through MATLAB/SIMULINK. Fig. 9 shows the soft starter and load motor used in the experiment. The load



**FIGURE 15.** The current waveforms when using the proposed method: (a)  $\gamma = 7$ , (b)  $\gamma = 5$ .

motor is equipped with an impeller and operates as a fan load. That is, the magnitude of the load torque increases with speed.

Fig. 10 shows the simulation results of speed command, speed, and current waveforms when  $\gamma = 2$ . It shows a case where  $\gamma$  is the same but has different current and speed response depending on the  $n$  value. Therefore, it is difficult to limit the current when using only the existing DFC method without a current controller.

Fig. 11 shows the simulation results of the rpm,  $\gamma$ , motor current, firing angle, and power used during startup when using the proposed method. The speed command increases according to the predetermined ramp time,  $t_r$ , and  $\gamma$  is calculated according to the speed command. Using this value, the  $\alpha_{ff}$  is compensated to the output of PI controller. The current limit value of 5A was used. When  $\gamma$  becomes 1, the feedforward value no longer changes, so it is started by the current controller. It can be seen that the proposed DFC method operates while effectively limiting the current magnitude because it uses an additional controller. In contrast, Fig. 12 shows simulation results using the existing phase control method. Likewise, the current was limited to 5A. The time it takes to complete startup is about 1.35 seconds, which is faster than the 1.7 seconds when using the proposed DFC method. However, when comparing the amount of power generated during the startup process, it can be seen that a larger loss occurs compared to the proposed method, at about 0.363Wh.

Fig. 13 shows the experimental results using the proposed DFC method. When the actual speed command,  $rpm^*$  rises, the  $\gamma$  is calculated to obtain the  $\alpha_{ff}$ . In addition to these  $\alpha_{ff}$  values, there is a PI controller that prevents overcurrent so the motor peak current is limited to  $i_{lim}$  during the startup process. Additionally, in the case of  $\gamma = 1$ , it can be confirmed that seamless transition occurs from the DFC to the phase control method. Conversely, Fig. 14 shows the experimental results when using the existing phase control method. Since the existing phase control method uses only a

current controller regardless of the speed command, the time it takes to start varies depending on the motor. The phase control method takes about 18 seconds, while the proposed DFC method takes 11 seconds to start. When using the proposed method, it was confirmed that faster startup time was required in the experiment, unlike in the simulation. This is presumed to be because there is an error in fan load conditions depending on the speed between simulation and experiment.

Fig. 15 shows the current waveforms at  $\gamma = 5$  and  $\gamma = 7$  when using the proposed method. As mentioned earlier, it can be seen that the turn-on point is determined according to the frequency division ratio  $\gamma$ , and the voltage of the divided frequency is applied to the motor. Comparing the current waveform, unlike the phase control method, there is a region where current does not flow, so the system efficiency improves during startup. This can be seen as similar to the two-phase conduction method of the predictive control. However, while the predictive control method requires motor speed and parameter information, the proposed DFC method can achieve similar performance by using only current information without motor parameter or speed.

## V. CONCLUSION

In this paper, a new discrete frequency control was proposed. Unlike the existing DFC method, an additional PI controller was used to limit the motor current. This is the same as the PI controller used in the phase control method. In this method, the speed command increases, a smooth transition occurs from the DFC method to the phase control method. This method increases system efficiency without additional structural changes or motor parameter information. Simulation and experimental results clearly demonstrate the effectiveness of the proposed method.

## REFERENCES

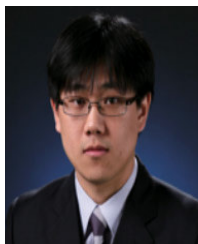
- [1] W. Jiang, X. Huang, J. Wang, J. Wang, and J. Li, "A carrier-based PWM strategy providing neutral-point voltage oscillation elimination for multi-phase neutral point clamped 3-level inverter," *IEEE Access*, vol. 7, pp. 124066–124076, 2019.
- [2] W. Lee, J. Kim, P. Jang, and K. Nam, "On-line MTPA control method for synchronous reluctance motor," *IEEE Trans. Ind. Appl.*, vol. 58, no. 1, pp. 356–364, Jan. 2022.
- [3] P. Yi, Y. Yin, X. Wang, X. Li, D. Chen, Y. Hu, and W. Ruan, "PMSM torque ripple minimization based on novel low carrier ratio PWM technique," *IEEE Trans. Power Electron.*, vol. 37, no. 9, pp. 11071–11084, Sep. 2022.
- [4] T. Sun, L. Long, R. Yang, K. Li, and J. Liang, "Extended virtual signal injection control for MTPA operation of IPMSM drives with online derivative term estimation," *IEEE Trans. Power Electron.*, vol. 36, no. 9, pp. 10602–10611, Sep. 2021.
- [5] A. Andersson and T. Thiringer, "Inverter losses minimization using variable switching frequency based on multi-objective optimization," in *Proc. Int. Conf. Electr. Mach. (ICEM)*, Sep. 2014, pp. 789–795.
- [6] J. Hang, H. Wu, S. Ding, Y. Huang, and W. Hua, "Improved loss minimization control for IPMSM using equivalent conversion method," *IEEE Trans. Power Electron.*, vol. 36, no. 2, pp. 1931–1940, Feb. 2021.
- [7] K. Li and Y. Wang, "Maximum torque per ampere (MTPA) control for IPMSM drives using signal injection and an MTPA control law," *IEEE Trans. Ind. Informat.*, vol. 15, no. 10, pp. 5588–5598, Oct. 2019.
- [8] S. F. Rabbi, J. T. Kahnemouei, X. Liang, and J. Yang, "Shaft failure analysis in soft-starter fed electrical submersible pump systems," *IEEE Open J. Ind. Appl.*, vol. 1, pp. 1–10, 2020.

- [9] I. A. Pires, A. A. P. Machado, and B. de Jesus Cardoso Filho, "Mitigation of electric arc furnace transformer inrush current using soft-starter-based controlled energization," *IEEE Trans. Ind. Appl.*, vol. 54, no. 4, pp. 3909–3918, Jul. 2018.
- [10] M. G. Solveson, B. Mirafzal, and N. A. O. Demerdash, "Soft-started induction motor modeling and heating issues for different starting profiles using a flux linkage ABC frame of reference," *IEEE Trans. Ind. Appl.*, vol. 42, no. 4, pp. 973–982, Jul. 2006.
- [11] G. Zenginobuz, I. Cadirci, M. Ermis, and C. Barlak, "Soft starting of large induction motors at constant current with minimized starting torque pulsations," *IEEE Trans. Ind. Appl.*, vol. 37, no. 5, pp. 1334–1347, 2001.
- [12] J. de Oliveira, A. Nied, R. P. Dias, and L. C. de Souza Marques, "Direct torque control of induction motor soft starting," in *Proc. Brazilian Power Electron. Conf.*, Sep. 2009, pp. 512–516.
- [13] H. Nannen, H. Zatocil, and G. Griepentrog, "Predictive firing algorithm for soft starter driven induction motors," *IEEE Trans. Ind. Electron.*, vol. 69, no. 12, pp. 12152–12161, Dec. 2022.
- [14] H. Nannen, H. Zatocil, and G. Griepentrog, "Industrialized flux-oriented starting algorithm for soft starter driven induction motors," in *Proc. 23rd Eur. Conf. Power Electron. Appl. (EPE ECCE Europe)*, Sep. 2021, pp. P.1–P.10.
- [15] A. Ginart, J. S. Camilleri, and G. Pesse, "Thyristor controlled AC induction motors using a discrete frequency control method," in *Proc. 29th Southeastern Symp. Syst. Theory*, 1997, pp. 164–167.
- [16] Z. Jiang, X. Huang, and N. Lin, "Simulation study of heavy motor soft starter based on discrete variable frequency," in *Proc. 4th Int. Conf. Comput. Sci. Educ.*, Jul. 2009, pp. 560–563.
- [17] Z. She, J. Liu, B. Zhang, and Y. Peng, "Research on high torque soft starter of induction motors based on discrete frequency," in *Proc. Int. Conf. Intell. Control Inf. Process.*, Aug. 2010, pp. 711–714.



**POOREUM JANG** was born in Yeosu-si, South Korea, in 1993. He received the B.S. degree in electrical engineering from Pusan National University, Pusan, South Korea, in 2017, and the M.S. and Ph.D. degrees in electrical engineering from the Pohang University of Science and Technology (POSTECH), Pohang, South Korea, in 2019 and 2022, respectively. Since 2023, he has been a Senior Research Engineer with the Korea Electronics Technology Institute (KETI),

Bucheon-si, South Korea. His current research interests include AC motor control, electric vehicle, and power converter.



**BYONG JO HYON** was born in South Korea, in 1984. He received the B.S. and M.S. degrees in electrical engineering from the Pohang University of Science and Technology, Pohang, South Korea, in 2010 and 2012, respectively. He is currently pursuing the Ph.D. degree in electrical engineering with Korea University, Seoul, South Korea. Since 2014, he has been a Senior Research Engineer with the Korea Electronics Technology Institute (KETI), Bucheon-si, South Korea. His research

interests include AC motor drive and LVDC energy conversion.



**DAE YEON HWANG** was born in Daegu, South Korea, in 1992. He received the B.S. and M.S. degrees in electrical engineering from Kyungpook National University, Daegu, in 2017 and 2019, respectively. He is currently pursuing the Ph.D. degree in electrical engineering with the Power Electronics Laboratory, Sungkyunkwan University. Since 2021, he has been a Senior Research Engineer with the Korea Electronics Technology Institute (KETI), Bucheon-si, South Korea. His current research interests include PMSM drive, multi-level inverter, and high efficiency systems.



**JOON SUNG PARK** was born in Seoul, South Korea, in 1978. He received the Ph.D. degree from the Department of Electrical Engineering, Hanyang University, Seoul, in 2018. From 2007 to 2009, he was with LG Electronics, Seoul. Since 2009, he has been a Principal Research Engineer with the Korea Electronics Technology Institute, Bucheon-si, South Korea. His current research interests include AC motor control, pulse width modulation converter, inverter

systems, and wave energy converter.



**JUN-HYUK CHOI** was born in Daegu, South Korea, in 1974. He received the Ph.D. degree from the School of Electrical and Electronic Engineering, Sungkyunkwan University, Suwon, South Korea, in 2003 and 2016, respectively. Since 2003, he has been a Principal Research Engineer with the Korea Electronics Technology Institute (KETI), Bucheon-si, South Korea. His research interests include power electronics and motor control systems.



**JIN-HONG KIM** was born in South Korea, in 1976. He received the B.S., M.S., and Ph.D. degree in electrical engineering from Sungkyunkwan University, Suwon, South Korea, in 2000, 2003, and 2016, respectively. From 2003 to 2010, he was a Researcher with LS Industrial Systems, South Korea. Since 2010, he has been a Principal Research Engineer with the Korea Electronics Technology Institute (KETI), Bucheon-si, South Korea. His research interests

include AC motor control, PWM converter/inverter systems, and electric energy conversions.

...